Observation of Three Charmoniumlike States with $J^{PC} = 1^{--}$ in $e^+e^- \to D^{*0}D^{*-}\pi^+$

M. Ablikim,[1] M. N. Achasov,[13,b] P. Adlarson,[73] R. Aliberti,[34] A. Amoroso,[72a,72c] M. R. An,[38] Q. An,[69,56] Y. Bai,[55] O. Bakina,[35] I. Balossino,[29a] Y. Ban,[45,g] V. Batozskaya,[1,43] K. Begzsuren,[31] N. Berger,[34] M. Bertani,[28a] D. Bettoni,[29a] F. Bianchi,[72a,72c] E. Bianco,[72a,72c] J. Bloms,[66] A. Bortone,[72a,72c] I. Boyko,[35] R. A. Briere,[5] A. Brueggemann,[66] H. Cai,[74] X. Cai,[1,56] A. Calcaterra,[28a] G. F. Cao,[1,61] N. Cao,[1,61] S. A. Cetin,[60a] J. F. Chang,[1,56] T. T. Chang,[75] W. L. Chang,[1,61] G. R. Che,[42] G. Chelkov,[35,a] C. Chen,[42] Chao Chen,[53] G. Chen,[1] H. S. Chen,[1,61] M. L. Chen,[1,56,61] S. J. Chen,[41] S. M. Chen,[59] T. Chen,[1,61] X. R. Chen,[30,61] X. T. Chen,[1,61] Y. B. Chen,[1,56] Y. Q. Chen,[33] Z. J. Chen,[25,h] W. S. Cheng,[72c] S. K. Choi,[10] X. Chu,[42] G. Cibinetto,[29a] S. C. Coen,[4] F. Cossio,[72c] J. J. Cui,[48] H. L. Dai,[1,56] J. P. Dai,[77] A. Dbeyssi,[19] R. E. de Boer,[4] D. Dedovich,[35] Z. Y. Deng,[1] A. Denig,[34] I. Denysenko,[35] M. Destefanis,[72a,72c] F. De Mori,[72a,72c] B. Ding,[64,1] X. X. Ding,[45,g] Y. Ding,[39] Y. Ding,[33] J. Dong,[1,56] L. Y. Dong,[1,61] M. Y. Dong,[1,56,61] X. Dong,[74] S. X. Du,[79] Z. H. Duan,[41] P. Egorov,[35,a] Y. L. Fan,[74] J. Fang,[1,56] S. S. Fang,[1,61] W. X. Fang,[1] Y. Fang,[1] R. Farinelli,[29a] L. Fava,[72b,72c] F. Feldbauer,[4] G. Felici,[28a] C. Q. Feng,[69,56] J. H. Feng,[57] K Fischer,[67] M. Fritsch,[4] C. Fritzsch,[66] C. D. Fu,[1] Y. W. Fu,[1] H. Gao,[61] Y. N. Gao,[45,g] Yang Gao,[69,56] S. Garbolino,[72c] I. Garzia,[29a,29b] P. T. Ge,[74] Z. W. Ge,[41] C. Geng,[57] E. M. Gersabeck,[65] A Gilman,[67] K. Goetzen,[14] L. Gong,[39] W. X. Gong,[1,56] W. Gradl,[34] S. Gramigna,[29a,29b] M. Greco,[72a,72c] M. H. Gu,[1,56] Y. T. Gu,[16] C. Y Guan,[1,61] Z. L. Guan,[22] A. Q. Guo,[30,61] L. B. Guo,[40] R. P. Guo,[47] Y. P. Guo,[12,f] A. Guskov,[35,a] X. T. H.,[1,61] W. Y. Han,[38] X. Q. Hao,[20] F. A. Harris,[63] K. K. He,[53] K. L. He,[1,61] F. H. Heinsius,[4] C. H. Heinz,[34] Y. K. Heng,[1,56,61] C. Herold,[58] T. Holtmann,[4] P. C. Hong,[12,f] G. Y. Hou,[1,61] Y. R. Hou,[61] Z. L. Hou,[1] H. M. Hu,[1,61] J. F. Hu,[54,i] T. Hu,[1,56,61] Y. Hu,[1] G. S. Huang,[69,56] K. X. Huang,[57] L. Q. Huang,[30,61] X. T. Huang,[48] Y. P. Huang,[1] T. Hussain,[71] N Hüsken,[27,34] W. Imoehl,[27] M. Irshad,[69,56] J. Jackson,[27] S. Jaeger,[4] S. Janchiv,[31] J. H. Jeong,[10] Q. Ji,[1] Q. P. Ji,[20] X. B. Ji,[1,61] X. L. Ji,[1,56] Y. Y. Ji,[48] Z. K. Jia,[69,56] P. C. Jiang,[45,g] S. S. Jiang,[38] T. J. Jiang,[17] X. S. Jiang,[1,56,61] Y. Jiang,[61] J. B. Jiao,[48] Z. Jiao,[23] S. Jin,[41] Y. Jin,[64] M. Q. Jing,[1,61] T. Johansson,[73] X. K.,[1] S. Kabana,[32] N. Kalantar-Nayestanaki,[62] X. L. Kang,[9] X. S. Kang,[39] R. Kappert,[62] M. Kavatsyuk,[62] B. C. Ke,[79] A. Khoukaz,[66] R. Kiuchi,[1] R. Kliemt,[14] L. Koch,[36] O. B. Kolcu,[60a] B. Kopf,[4] M. Kuessner,[4] A. Kupsc,[43,73] W. Kühn,[36] J. J. Lane,[65] J. S. Lange,[36] P. Larin,[19] A. Lavania,[26] L. Lavezzi,[72a,72c] T. T. Lei,[69,k] Z. H. Lei,[69,56] H. Leithoff,[34] M. Lellmann,[34] T. Lenz,[34] C. Li,[46] C. Li,[42] C. H. Li,[38] Cheng Li,[69,56] D. M. Li,[79] F. Li,[1,56] G. Li,[1] H. Li,[69,56] H. B. Li,[1,61] H. J. Li,[20] H. N. Li,[54,i] Hui Li,[42] J. R. Li,[59] J. S. Li,[57] J. W. Li,[48] Ke Li,[1] L. J Li,[1,61] L. K. Li,[1] Lei Li,[3] M. H. Li,[42] P. R. Li,[37,j,k] S. X. Li,[12] T. Li,[48] W. D. Li,[1,61] W. G. Li,[1] X. H. Li,[69,56] X. L. Li,[48] Xiaoyu Li,[1,61] Y. G. Li,[45,g] Z. J. Li,[57] Z. X. Li,[16] Z. Y. Li,[57] C. Liang,[41] H. Liang,[69,56] H. Liang,[33] H. Liang,[1,61] Y. F. Liang,[52] Y. T. Liang,[30,61] G. R. Liao,[15] L. Z. Liao,[48] J. Libby,[26] A. Limphirat,[58] D. X. Lin,[30,61] T. Lin,[1] B. X. Liu,[74] B. J. Liu,[1] C. Liu,[33] C. X. Liu,[1] D. Liu,[19,69] F. H. Liu,[51] Fang Liu,[1] Feng Liu,[6] G. M. Liu,[54,i] H. Liu,[37,j,k] H. B. Liu,[16] H. M. Liu,[1,61] Huanhuan Liu,[1] Huihui Liu,[21] J. B. Liu,[69,56] J. L. Liu,[70] J. Y. Liu,[1,61] K. Liu,[1] K. Y. Liu,[39] Ke Liu,[22] L. Liu,[69,56] L. C. Liu,[42] Lu Liu,[42] M. H. Liu,[12,f] P. L. Liu,[1] Q. Liu,[61] S. B. Liu,[69,56] T. Liu,[12,f] W. K. Liu,[42] W. M. Liu,[69,56] X. Liu,[37,j,k] Y. Liu,[37,j,k] Y. B. Liu,[42] Z. A. Liu,[1,56,61] Z. Q. Liu,[48] X. C. Lou,[1,56,61] F. X. Lu,[57] H. J. Lu,[23] J. G. Lu,[1,56] X. L. Lu,[1] Y. Lu,[7] Y. P. Lu,[1,56] Z. H. Lu,[1,61] C. L. Luo,[40] M. X. Luo,[78] T. Luo,[12,f] X. L. Luo,[1,56] X. R. Lyu,[61] Y. F. Lyu,[42] F. C. Ma,[39] H. L. Ma,[1] J. L. Ma,[1,61] L. L. Ma,[48] M. M. Ma,[1,61] Q. M. Ma,[1] R. Q. Ma,[1,61] R. T. Ma,[61] X. Y. Ma,[1,56] Y. Ma,[45,g] F. E. Maas,[19] M. Maggiora,[72a,72c] S. Maldaner,[4] S. Malde,[67] A. Mangoni,[28b] Y. J. Mao,[45,g] Z. P. Mao,[1] S. Marcello,[72a,72c] Z. X. Meng,[64] J. G. Messchendorp,[14,62] G. Mezzadri,[29a] H. Miao,[1,61] T. J. Min,[41] R. E. Mitchell,[27] X. H. Mo,[1,56,61] N. Yu. Muchnoi,[13,b] Y. Nefedov,[35] F. Nerling,[19,d] I. B. Nikolaev,[13,b] Z. Ning,[1,56] S. Nisar,[11,l] Y. Niu,[48] S. L. Olsen,[61] Q. Ouyang,[1,56,61] S. Pacetti,[28b,28c] X. Pan,[53] Y. Pan,[55] A. Pathak,[33] Y. P. Pei,[69,56] M. Pelizaeus,[4] H. P. Peng,[69,56] K. Peters,[14,d] J. L. Ping,[40] R. G. Ping,[1,61] S. Plura,[34] S. Pogodin,[35] V. Prasad,[32] F. Z. Qi,[1] H. Qi,[69,56] H. R. Qi,[59] M. Qi,[41] T. Y. Qi,[12,f] S. Qian,[1,56] W. B. Qian,[61] C. F. Qiao,[61] J. J. Qin,[70] L. Q. Qin,[15] X. P. Qin,[12,f] X. S. Qin,[48] Z. H. Qin,[1,56] J. F. Qiu,[1] S. Q. Qu,[59] C. F. Redmer,[34] K. J. Ren,[38] A. Rivetti,[72c] V. Rodin,[62] M. Rolo,[72c] G. Rong,[1,61] Ch. Rosner,[19] S. N. Ruan,[42] N. Salone,[43] A. Sarantsev,[35,c] Y. Schelhaas,[34] K. Schoenning,[73] M. Scodeggio,[29a,29b] K. Y. Shan,[12,f] W. Shan,[24] X. Y. Shan,[69,56] J. F. Shangguan,[53] L. G. Shao,[1,61] M. Shao,[69,56] C. P. Shen,[12,f] H. F. Shen,[1,61] W. H. Shen,[61] X. Y. Shen,[1,61] B. A. Shi,[61] H. C. Shi,[69,56] J. Y. Shi,[1] Q. Q. Shi,[53] R. S. Shi,[1,61] X. Shi,[1,56] J. J. Song,[20] T. Z. Song,[57] W. M. Song,[33,1] Y. X. Song,[45,g] S. Sosio,[72a,72c] S. Spataro,[72a,72c] F. Stieler,[34] Y. J. Su,[61] G. B. Sun,[74] G. X. Sun,[1] H. Sun,[61] H. K. Sun,[1] J. F. Sun,[20] K. Sun,[59] L. Sun,[74] S. S. Sun,[1,61] T. Sun,[1,61] W. Y. Sun,[33] Y. Sun,[9] Y. J. Sun,[69,56] Y. Z. Sun,[1] Z. T. Sun,[48] Y. X. Tan,[69,56] C. J. Tang,[52] G. Y. Tang,[1] J. Tang,[57] Y. A. Tang,[74] L. Y Tao,[70] Q. T. Tao,[25,h] M. Tat,[67] J. X. Teng,[69,56] V. Thoren,[73] W. H. Tian,[57] W. H. Tian,[50] Y. Tian,[30,61] Z. F. Tian,[74] I. Uman,[60b] B. Wang,[1] B. L. Wang,[61] Bo Wang,[69,56] C. W. Wang,[41] D. Y. Wang,[45,g] F. Wang,[70] H. J. Wang,[37,j,k] H. P. Wang,[1,61] K. Wang,[1,56] L. L. Wang,[1] M. Wang,[48] Meng Wang,[1,61] S. Wang,[12,f] T. Wang,[12,f] T. J. Wang,[42] W. Wang,[57]

W. Wang,[70] W. H. Wang,[74] W. P. Wang,[69,56] X. Wang,[45,g] X. F. Wang,[37,j,k] X. J. Wang,[38] X. L. Wang,[12,f] Y. Wang,[59] Y. D. Wang,[44] Y. F. Wang,[1,56,61] Y. H. Wang,[46] Y. N. Wang,[44] Y. Q. Wang,[1] Yaqian Wang,[18,1] Yi Wang,[59] Z. Wang,[1,56] Z. L. Wang,[70] Z. Y. Wang,[1,61] Ziyi Wang,[61] D. Wei,[68] D. H. Wei,[15] F. Weidner,[66] S. P. Wen,[1] C. W. Wenzel,[4] U. Wiedner,[4] G. Wilkinson,[67] M. Wolke,[73] L. Wollenberg,[4] C. Wu,[38] J. F. Wu,[1,61] L. H. Wu,[1] L. J. Wu,[1,61] X. Wu,[12,f] X. H. Wu,[33] Y. Wu,[69] Y. J Wu,[30] Z. Wu,[1,56] L. Xia,[69,56] X. M. Xian,[38] T. Xiang,[45,g] D. Xiao,[37,j,k] G. Y. Xiao,[41] H. Xiao,[12,f] S. Y. Xiao,[1] Y. L. Xiao,[12,f] Z. J. Xiao,[40] C. Xie,[41] X. H. Xie,[45,g] Y. Xie,[48] Y. G. Xie,[1,56] Y. H. Xie,[6] Z. P. Xie,[69,56] T. Y. Xing,[1,61] C. F. Xu,[1,61] C. J. Xu,[57] G. F. Xu,[1] H. Y. Xu,[64] Q. J. Xu,[17] W. L. Xu,[64] X. P. Xu,[53] Y. C. Xu,[76] Z. P. Xu,[41] Z. S. Xu,[61] F. Yan,[12,f] L. Yan,[12,f] W. B. Yan,[69,56] W. C. Yan,[79] X. Q Yan,[1] H. J. Yang,[49,e] H. L. Yang,[33] H. X. Yang,[1] Tao Yang,[1] Y. Yang,[12,f] Y. F. Yang,[42] Y. X. Yang,[1,61] Yifan Yang,[1,61] M. Ye,[1,56] M. H. Ye,[8] J. H. Yin,[1] Z. Y. You,[57] B. X. Yu,[1,56,61] C. X. Yu,[42] G. Yu,[1,61] T. Yu,[70] X. D. Yu,[45,g] C. Z. Yuan,[1,61] L. Yuan,[2] S. C. Yuan,[1] X. Q. Yuan,[1] Y. Yuan,[1,61] Z. Y. Yuan,[57] C. X. Yue,[38] A. A. Zafar,[71] F. R. Zeng,[48] X. Zeng,[12,f] Y. Zeng,[25,h] Y. J. Zeng,[1,61] X. Y. Zhai,[33] Y. H. Zhan,[57] A. Q. Zhang,[1,61] B. L. Zhang,[1,61] B. X. Zhang,[1] D. H. Zhang,[42] G. Y. Zhang,[20] H. Zhang,[69] H. H. Zhang,[33] H. H. Zhang,[57] H. Q. Zhang,[1,56,61] H. Y. Zhang,[1,56] J. J. Zhang,[50] J. L. Zhang,[75] J. Q. Zhang,[40] J. W. Zhang,[1,56,61] J. X. Zhang,[37,j,k] J. Y. Zhang,[1] J. Z. Zhang,[1,61] Jiawei Zhang,[1,61] L. M. Zhang,[59] L. Q. Zhang,[57] Lei Zhang,[41] P. Zhang,[1] Q. Y. Zhang,[38,79] Shuihan Zhang,[1,61] Shulei Zhang,[25,h] X. D. Zhang,[44] X. M. Zhang,[1] X. Y. Zhang,[53] X. Y. Zhang,[48] Y. Zhang,[67] Y. T. Zhang,[79] Y. H. Zhang,[1,56] Yan Zhang,[69,56] Yao Zhang,[1] Z. H. Zhang,[1] Z. L. Zhang,[33] Z. Y. Zhang,[74] Z. Y. Zhang,[42] G. Zhao,[1] J. Zhao,[38] J. Y. Zhao,[1,61] J. Z. Zhao,[1,56] Lei Zhao,[69,56] Ling Zhao,[1] M. G. Zhao,[42] S. J. Zhao,[79] Y. B. Zhao,[1,56] Y. X. Zhao,[30,61] Z. G. Zhao,[69,56] A. Zhemchugov,[35,a] B. Zheng,[70] J. P. Zheng,[1,56] W. J. Zheng,[1,61] Y. H. Zheng,[61] B. Zhong,[40] X. Zhong,[57] H. Zhou,[48] L. P. Zhou,[1,61] X. Zhou,[74] X. K. Zhou,[6] X. R. Zhou,[69,56] X. Y. Zhou,[38] Y. Z. Zhou,[12,f] J. Zhu,[42] K. Zhu,[1] K. J. Zhu,[1,56,61] L. Zhu,[33] L. X. Zhu,[61] S. H. Zhu,[68] S. Q. Zhu,[41] T. J. Zhu,[12,f] W. J. Zhu,[12,f] Y. C. Zhu,[69,56] Z. A. Zhu,[1,61] J. H. Zou,[1] and J. Zu[69,56]

(BESIII Collaboration)

[1]*Institute of High Energy Physics, Beijing 100049, People's Republic of China*
[2]*Beihang University, Beijing 100191, People's Republic of China*
[3]*Beijing Institute of Petrochemical Technology, Beijing 102617, People's Republic of China*
[4]*Bochum Ruhr-University, D-44780 Bochum, Germany*
[5]*Carnegie Mellon University, Pittsburgh, Pennsylvania 15213, USA*
[6]*Central China Normal University, Wuhan 430079, People's Republic of China*
[7]*Central South University, Changsha 410083, People's Republic of China*
[8]*China Center of Advanced Science and Technology, Beijing 100190, People's Republic of China*
[9]*China University of Geosciences, Wuhan 430074, People's Republic of China*
[10]*Chung-Ang University, Seoul, 06974, Republic of Korea*
[11]*COMSATS University Islamabad, Lahore Campus, Defence Road, Off Raiwind Road, 54000 Lahore, Pakistan*
[12]*Fudan University, Shanghai 200433, People's Republic of China*
[13]*G.I. Budker Institute of Nuclear Physics SB RAS (BINP), Novosibirsk 630090, Russia*
[14]*GSI Helmholtzcentre for Heavy Ion Research GmbH, D-64291 Darmstadt, Germany*
[15]*Guangxi Normal University, Guilin 541004, People's Republic of China*
[16]*Guangxi University, Nanning 530004, People's Republic of China*
[17]*Hangzhou Normal University, Hangzhou 310036, People's Republic of China*
[18]*Hebei University, Baoding 071002, People's Republic of China*
[19]*Helmholtz Institute Mainz, Staudinger Weg 18, D-55099 Mainz, Germany*
[20]*Henan Normal University, Xinxiang 453007, People's Republic of China*
[21]*Henan University of Science and Technology, Luoyang 471003, People's Republic of China*
[22]*Henan University of Technology, Zhengzhou 450001, People's Republic of China*
[23]*Huangshan College, Huangshan 245000, People's Republic of China*
[24]*Hunan Normal University, Changsha 410081, People's Republic of China*
[25]*Hunan University, Changsha 410082, People's Republic of China*
[26]*Indian Institute of Technology Madras, Chennai 600036, India*
[27]*Indiana University, Bloomington, Indiana 47405, USA*
[28a]*INFN Laboratori Nazionali di Frascati, INFN Laboratori Nazionali di Frascati, I-00044, Frascati, Italy*
[28b]*INFN Sezione di Perugia, I-06100, Perugia, Italy*
[28c]*University of Perugia, I-06100, Perugia, Italy*
[29a]*INFN Sezione di Ferrara, INFN Sezione di Ferrara, I-44122, Ferrara, Italy*
[29b]*University of Ferrara, I-44122, Ferrara, Italy*
[30]*Institute of Modern Physics, Lanzhou 730000, People's Republic of China*

[31]Institute of Physics and Technology, Peace Avenue 54B, Ulaanbaatar 13330, Mongolia
[32]Instituto de Alta Investigación, Universidad de Tarapacá, Casilla 7D, Arica, Chile
[33]Jilin University, Changchun 130012, People's Republic of China
[34]Johannes Gutenberg University of Mainz, Johann-Joachim-Becher-Weg 45, D-55099 Mainz, Germany
[35]Joint Institute for Nuclear Research, 141980 Dubna, Moscow region, Russia
[36]Justus-Liebig-Universitaet Giessen, II. Physikalisches Institut, Heinrich-Buff-Ring 16, D-35392 Giessen, Germany
[37]Lanzhou University, Lanzhou 730000, People's Republic of China
[38]Liaoning Normal University, Dalian 116029, People's Republic of China
[39]Liaoning University, Shenyang 110036, People's Republic of China
[40]Nanjing Normal University, Nanjing 210023, People's Republic of China
[41]Nanjing University, Nanjing 210093, People's Republic of China
[42]Nankai University, Tianjin 300071, People's Republic of China
[43]National Centre for Nuclear Research, Warsaw 02-093, Poland
[44]North China Electric Power University, Beijing 102206, People's Republic of China
[45]Peking University, Beijing 100871, People's Republic of China
[46]Qufu Normal University, Qufu 273165, People's Republic of China
[47]Shandong Normal University, Jinan 250014, People's Republic of China
[48]Shandong University, Jinan 250100, People's Republic of China
[49]Shanghai Jiao Tong University, Shanghai 200240, People's Republic of China
[50]Shanxi Normal University, Linfen 041004, People's Republic of China
[51]Shanxi University, Taiyuan 030006, People's Republic of China
[52]Sichuan University, Chengdu 610064, People's Republic of China
[53]Soochow University, Suzhou 215006, People's Republic of China
[54]South China Normal University, Guangzhou 510006, People's Republic of China
[55]Southeast University, Nanjing 211100, People's Republic of China
[56]State Key Laboratory of Particle Detection and Electronics, Beijing 100049, Hefei 230026, People's Republic of China
[57]Sun Yat-Sen University, Guangzhou 510275, People's Republic of China
[58]Suranaree University of Technology, University Avenue 111, Nakhon Ratchasima 30000, Thailand
[59]Tsinghua University, Beijing 100084, People's Republic of China
[60a]Turkish Accelerator Center Particle Factory Group, Istinye University, 34010, Istanbul, Turkey
[60b]Near East University, Nicosia, North Cyprus, 99138, Mersin 10, Turkey
[61]University of Chinese Academy of Sciences, Beijing 100049, People's Republic of China
[62]University of Groningen, NL-9747 AA Groningen, Netherlands
[63]University of Hawaii, Honolulu, Hawaii 96822, USA
[64]University of Jinan, Jinan 250022, People's Republic of China
[65]University of Manchester, Oxford Road, Manchester, M13 9PL, United Kingdom
[66]University of Muenster, Wilhelm-Klemm-Strasse 9, 48149 Muenster, Germany
[67]University of Oxford, Keble Road, Oxford OX13RH, United Kingdom
[68]University of Science and Technology Liaoning, Anshan 114051, People's Republic of China
[69]University of Science and Technology of China, Hefei 230026, People's Republic of China
[70]University of South China, Hengyang 421001, People's Republic of China
[71]University of the Punjab, Lahore-54590, Pakistan
[72a]University of Turin and INFN, University of Turin, I-10125, Turin, Italy
[72b]University of Eastern Piedmont, I-15121, Alessandria, Italy
[72c]INFN, I-10125, Turin, Italy
[73]Uppsala University, Box 516, SE-75120 Uppsala, Sweden
[74]Wuhan University, Wuhan 430072, People's Republic of China
[75]Xinyang Normal University, Xinyang 464000, People's Republic of China
[76]Yantai University, Yantai 264005, People's Republic of China
[77]Yunnan University, Kunming 650500, People's Republic of China
[78]Zhejiang University, Hangzhou 310027, People's Republic of China
[79]Zhengzhou University, Zhengzhou 450001, People's Republic of China

(Received 18 January 2023; revised 16 February 2023; accepted 24 February 2023; published 23 March 2023)

The Born cross sections of the process $e^+e^- \to D^{*0}D^{*-}\pi^+$ at center-of-mass energies from 4.189 to 4.951 GeV are measured for the first time. The data samples used correspond to an integrated luminosity of 17.9 fb^{-1} and were collected by the BESIII detector operating at the BEPCII storage ring. Three enhancements around 4.20, 4.47, and 4.67 GeV are visible. The resonances have masses of $4209.6 \pm 4.7 \pm 5.9$ MeV/c^2, $4469.1 \pm 26.2 \pm 3.6$ MeV/c^2, and $4675.3 \pm 29.5 \pm 3.5$ MeV/c^2 and widths of $81.6 \pm 17.8 \pm 9.0$ MeV, $246.3 \pm 36.7 \pm 9.4$ MeV, and $218.3 \pm 72.9 \pm 9.3$ MeV, respectively, where the first uncertainties are statistical and the second systematic. The first and third resonances are consistent with the $\psi(4230)$ and $\psi(4660)$ states, respectively, while the second one is compatible with the $\psi(4500)$ observed in the $e^+e^- \to K^+K^-J/\psi$ process. These three charmoniumlike ψ states are observed in the $e^+e^- \to D^{*0}D^{*-}\pi^+$ process for the first time.

DOI: 10.1103/PhysRevLett.130.121901

The standard model of particle physics describes how quarks interact with each other to create various states of matter and antimatter. Over the past years, a series of charmoniumlike vector meson ψ states (also denoted as Y), containing at least $c\bar{c}$ quark pairs, have been observed via electron-positron annihilation in numerous experiments [1]. Dedicated studies of these charmoniumlike states, which have unit spin and negative charge-parity quantum numbers $J^{PC} = 1^{--}$, were initially triggered by the discovery of the $\psi(4230)$, previously called the $\psi(4260)$, in the $e^+e^- \to \pi^+\pi^- J/\psi$ process at *BABAR* [2], which was confirmed at CLEO [3], Belle [4], and BESIII [5–7]. Later, the $\psi(4360)$ and $\psi(4660)$ states were established in $e^+e^- \to \pi^+\pi^-\psi(2S)$ at *BABAR* [8,9], Belle [10,11], and BESIII [12–14]. Some similar resonance enhancements around 4.23 GeV, 4.36 GeV, or 4.66 GeV are also reported in $\pi^+\pi^- h_c$ [15], $\omega\chi_{c0}$ [16,17], $\eta J/\psi$ [18], $\eta' J/\psi$ [19], $D^0D^{*-}\pi^+$ [20], $\pi\pi\psi_2(3823)$ [21], $\pi^+\pi^- D^+D^-$ [22,23], and K^+K^-J/ψ [24] final states at BESIII. In addition, a new ψ state, the $\psi(4500)$, was observed in $e^+e^- \to K^+K^-J/\psi$, recently [24]. The genuine properties of these charmoniumlike ψ states are still unknown, and there exist various theoretical interpretations, including tetraquarks, hybrid mesons, hadron molecules, hadrocharmonium, vector charmonia, and threshold effects [25,26].

One striking feature of these charmoniumlike states is their large coupling to charmonium final states [27]. In contrast, there is a dip around the known $\psi(4230)$ mass in the cross section of $e^+e^- \to$ inclusive hadrons [28] and in the exclusive two-body production of $e^+e^- \to D^{(*)}\bar{D}^{(*)}$ [29,30]. This is opposite to the behavior of conventional $c\bar{c}$ charmonium states lying above the $D\bar{D}$ mass threshold, which predominantly decays to open-charm final states [1]. Therefore, it is essential to investigate the coupling of the charmoniumlike states to different open-charm channels to help identify their nature.

In the process $e^+e^- \to D^0D^{*-}\pi^+$ [20], BESIII first determined a sizable coupling of the $\psi(4230)$ with the open-charm $D^0D^{*-}\pi^+$ decay, which is consistent with the hypothesis of a $D_1(2420)\bar{D}$ molecular state [31–37]. In lattice QCD, the leptonic partial width $\Gamma^{ee}_{\psi(4230)}$ of the $\psi(4230)$ is predicted to be less than 40 eV using a hybrid scenario [38]. To date, $\Gamma^{ee}_{\psi(4230)}$ is evaluated to be 36.4 ± 4.7 eV, based on the combined analysis of the known $\psi(4230)$ decay channels [39]. Study of the $\psi(4230)$ in the open-charm process $e^+e^- \to D^*\bar{D}^*\pi$ provides new input to $\Gamma^{ee}_{\psi(4230)}$ and to the relative size of different decay modes, which can be used to test the theoretical explanation of the hybrid and $D\bar{D}_1$ molecular state models.

The $\psi(4500)$ is reported in the $e^+e^- \to K^+K^-J/\psi$ process [24]. Its spin-parity and mass agree with the lattice QCD calculation for a $c\bar{c}s\bar{s}$ tetraquark state [40]; a baryonium state [41]; a $D^*\bar{D}_2$ molecule state [42]; a hidden-charm tetraquark candidate in QCD sum rule [43]; a $D_s\bar{D}_{s1}$ molecule state [42,44], which is a hidden-strangeness partner of the $\psi(4230)$ state under the $D\bar{D}_1$ molecule assumption [44]; and a vector charmonium $5S$-$4D$ mixing state [45]. To explore its true nature, an independent confirmation of the $\psi(4500)$ in another channel would be important and crucial. In addition, since the Born cross section of $e^+e^- \to KZ_{cs}(3985)$ peaks around the $\psi(4660)$ mass [46,47], the $\psi(4660)$ is considered to be a hidden-strangeness state. Given that the heavier $\psi(4500)$ and $\psi(4660)$ states have not been observed in open-charm decay, it is also highly desirable to explore these states in the process $e^+e^- \to D^*\bar{D}^*\pi$ to help determine their quark constituents.

In this Letter, the Born cross sections of the $e^+e^- \to D^{*0}D^{*-}\pi^+$ processes are measured at 86 center-of-mass energies from 4.189 to 4.951 GeV for the first time. Charge conjugate modes are always implied throughout this Letter. The datasets used are accumulated with the BESIII detector at the BEPCII collider and correspond to an integrated luminosity of 17.9 fb^{-1} [48–50]. Details about BEPCII and BESIII can be found in Refs. [51–53]. The datasets include 49 energy points with integrated luminosities less than 10 pb^{-1} ("scan data") and another 37 energy points with larger integrated luminosities ("*XYZ* data"). Details of the datasets can be found in Tables I and II of the Supplemental Material [54]. By fitting the line shape of dressed cross sections, which takes into account vacuum polarizations [58], we report the observation of three vector charmoniumlike ψ states in $e^+e^- \to D^{*0}D^{*-}\pi^+$.

Simulated data samples are produced with GEANT4-based [59] Monte Carlo (MC) software, which includes the geometric description [60] of the BESIII detector and the detector response, as detailed in Ref. [53]. The simulation models the beam energy spread and initial state radiation (ISR) in the e^+e^- annihilation with the generator KKMC [61]. The signal MC samples of the $e^+e^- \to D^{*0}D^{*-}\pi^+$ process are generated according to the partial-wave-analysis results at each energy point. Possible background contributions are estimated by inclusive MC simulation samples, which include the production of open-charm processes, the ISR production of vector charmonium(like) states, and the continuum processes incorporated in KKMC. All particle decays are modeled with EVTGEN [62] using branching fractions (BFs) taken from the Particle Data Group (PDG) [1], when available, and unknown J/ψ and $\psi(2S)$ decays are estimated with LUNDCHARM [63]. Final state radiation from charged final state particles is incorporated using PHOTOS [64].

To improve the signal selection efficiency, a partial-reconstruction technique is employed to identify the $D^{*0}D^{*-}\pi^+$ final states, in which two tagging methods, the D^0 tag and the D^- tag, are performed. In the $D^0(D^-)$-tag method, the bachelor charged π^+ from primary production, the $D^0(D^-)$ meson, and at least one soft $\pi^0(\to\gamma\gamma)$ from $D^{*0}(D^{*-}) \to D^0(D^-)\pi^0$ decay are reconstructed. To improve the signal purity, only the decays $D^0 \to K^-\pi^+$, $K^-\pi^+\pi^0$, and $K^-\pi^+\pi^+\pi^-$ ($D^- \to K^+\pi^-\pi^-$), which have relatively large BFs, are reconstructed. By reconstructing the $D^{*0}(D^{*-})$ and the bachelor π^+, the flavor of the missing $D^{*-}(D^{*0})$ meson is fixed. All the charged tracks and π^0 candidates are selected following the criteria in Ref. [65]. To form candidates for $D^0 \to K^-\pi^+$, $D^0 \to K^-\pi^+\pi^0$, $D^0 \to K^-\pi^+\pi^+\pi^-$, and $D^- \to K^+\pi^-\pi^-$ decays, the reconstructed final state invariant masses are required to be within (1.835,1.887), (1.827,1.882), (1.855,1.874), and $(1.856, 1.883)$ GeV/c^2, respectively. Here, the different mass regions are due to the various momentum resolutions. The π^0 candidates from D^* decays can be either from the reconstructed or missing D^* candidates. For the π^0 from missing D^* candidates, its momentum in the reconstructed $D\pi^+$ recoil system, $P^*(\pi^0)$, peaks around 40 MeV/c. To distinguish the source of π^0 with reconstructed D^* candidates, the reconstructed invariant masses are required to satisfy $M(D^0\pi^0) \in (2.004, 2.009)$ GeV/c^2 with $P^*(\pi^0) \notin (0.025, 0.050)$ GeV/c in the D^0 tag method, and $M(D^-\pi^0) \in (2.008, 2.013)$ GeV/c^2 with $P^*(\pi^0) \notin (0.030, 0.055)$ GeV/c in the D^- tag method, as shown in Fig. 1 for data at $\sqrt{s} = 4.600$ GeV. Moreover, the π^+D^0 invariant mass must be greater than 2.02 GeV/c^2 in the D^0 tag method to reject background for the bachelor π^+ from $D^{*+} \to \pi^+D^0$.

To improve the resolution and further suppress the background, a kinematic fit (3C) is performed to constrain the reconstructed π^0, $D^0(D^-)$, and $D^{*0}(D^{*-})$ mesons to their individual known masses [1]. Candidate events are required to have $\chi^2_{\rm 3C} < 50$ and the fitted four-momenta of all related particles are used for further analysis. If there is more than one $\pi^0D^0(D^-)$ candidate in an event, only the one with the minimum $\chi^2_{\rm 3C}$ is retained. Furthermore, if one event survives in both tag methods, only the combination in the D^0-tag method is kept to avoid double counting in the simultaneous fit.

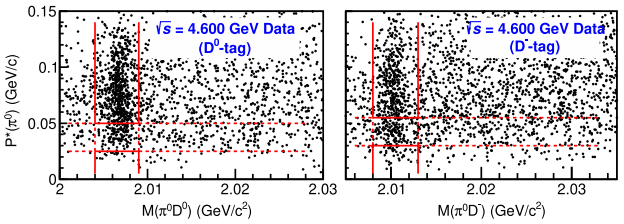

FIG. 1. Two-dimensional distributions of $P^*(\pi^0)$ versus $M(\pi^0D)$ for the D^0-tag (left) and D^--tag (right) methods in data at $\sqrt{s} = 4.600$ GeV. The events between the vertical solid lines are kept, and those between the horizontal dashed lines are vetoed based on the requirements for $M(\pi^0D)$ and $P^*(\pi^0)$. The distributions for signal MC simulation samples are shown in Fig. 1 of the Supplemental Material [54].

Figure 2 shows the distributions of the recoil masses of reconstructed π^+, π^0, and D mesons, $RM(\pi^+\pi^0D^0)$ and $RM(\pi^+\pi^0D^-)$. The background study based on inclusive MC simulation samples shows that the shape of the background at each energy point is smooth and can be well described by a second-order Chebyshev function. A peaking background is found in the signal MC simulation due to the miscombination of particles from the missing and tagged sides. Its shape is obtained by selecting the unmatched events from inclusive MC simulation samples, in which the missing D^* candidate decays inclusively while the tagged D^* candidate decays into the signal process final state. Its contribution is fixed in the fit according to the ratio between matched and unmatched events in the MC simulation.

An unbinned extended maximum likelihood fit is performed on the distributions of $RM(\pi^+\pi^0D^0)$ and $RM(\pi^+\pi^0D^-)$ simultaneously to determine the Born cross section at each energy point. Figure 2 shows the fit results at $\sqrt{s} = 4.600$ GeV, as an example. The signal shape is

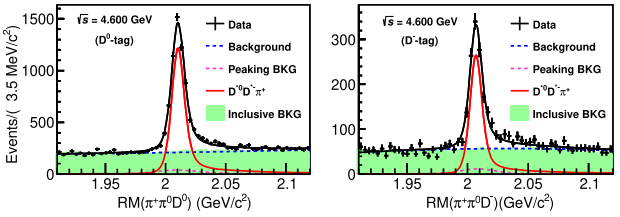

FIG. 2. The distributions of the recoil masses $RM(\pi^+\pi^0D^0)$ (left) and $RM(\pi^+\pi^0D^-)$ (right) for data at $\sqrt{s} = 4.600$ GeV with simultaneous fit results overlaid. The red solid-curve is the signal shape. The pink and blue dashed-curve are the peaking and smooth background, respectively. The light green shadowed histogram is the simulated inclusive background MC samples.

derived from MC simulation convolved with a Gaussian function with free parameters to account for the resolution difference between data and MC simulation. The background shape is parametrized as a sum of the shape from unmatched MC samples and a second-order Chebyshev function. The Born cross sections ($\sigma^{\rm Born}$) at the individual energy points are defined as

$$\sigma^{\rm Born} = \frac{\sigma^{\rm dressed}}{\frac{1}{|1-\Pi|^2}} = \frac{N^{\rm obs}_{D^{0(-)}\text{-tag}}}{\mathcal{L}_{\rm int}\,\epsilon_{D^{0(-)}\text{-tag}}\,\hat{\mathcal{B}}_{D^{0(-)}\text{-tag}}\,(1+\delta^{\rm ISR})\,\frac{1}{|1-\Pi|^2}}.$$

Here, $N^{\rm obs}_{D^{0(-)}\text{-tag}}$ is calculated according to $\sigma^{\rm Born}$ which is taken as a common parameter in the simultaneous fit, $\epsilon_{D^{0(-)}\text{-tag}}$ is the detection efficiency, $\mathcal{L}_{\rm int}$ is the integral luminosity measured by Refs. [48–50], $\hat{\mathcal{B}}_{D^{0(-)}\text{-tag}}$ stands for an equivalent BF including all the related products of the BF obtained from the PDG [1], while $(1+\delta^{\rm ISR})$ and $(1/|1-\Pi|^2)$ are the correction factors for ISR and vacuum polarization [66]. To estimate the ISR factors and consider the correlation effect on detection efficiencies, an iterative weighting method [67] is performed to correct the corresponding dressed cross section values. All the numerical results from the fits are summarized in Tables I and II of the Supplemental Material [54] for the XYZ and scan data samples, respectively.

The systematic uncertainties in the Born cross section measurements, as detailed in the Supplemental Material [54], are divided into three parts. The first part relates to the determination of the detection efficiency, including the tracking, particle identification, π^0 reconstruction, signal region requirements, signal decay model, and ISR correction factor. The second part relates to the estimation of signal yields from the fit, consisting of the signal and background shapes as well as the fit range. The last part includes the uncertainties from the luminosities and the intermediate BFs. The items in the first and third parts are completely correlated between different energy points, except for the uncertainties due to signal region requirements and the signal decay model. For the second part at low-yield (<300 events) energy points, the systematic uncertainties obtained at their nearest energy point in high-yield (>300 events) XYZ data are used. All the systematic uncertainties are studied for each tag method and combined to obtain the total systematic uncertainties according to their signal yields. The total relative systematic uncertainties at different energy points are between 6.7 and 9.6%.

The dressed cross sections obtained at various energy points are shown in Fig. 3. Three possible enhancements around 4.20, 4.47, and 4.67 GeV are observed. To fit this line shape, we use the coherent sum of a continuum amplitude for $e^+e^- \to D^{*0}D^{*-}\pi^+$ and three resonance

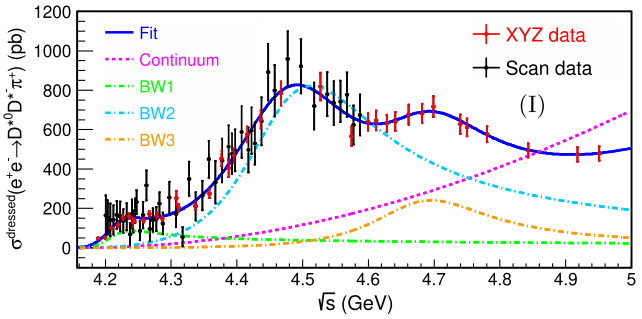

FIG. 3. The fit results (solution I) of the dressed cross section line shape of $e^+e^- \to D^{*0}D^{*-}\pi^+$. The black and red points with error bars are data, including statistical and systematic uncertainties. The blue curve is the total fit. The green, azure, and orange dashed curves describe three BW functions, and the pink dashed curve is the three body phase space contribution.

amplitudes described by relativistic Breit-Wigner (BW) functions

$$\sigma^{\rm dressed}(\sqrt{s}) = C_0\left|C_1\sqrt{\Phi(\sqrt{s})} + \sum_{k=1}^{3}{\rm BW}_k(\sqrt{s})e^{i\phi_k}\right|^2,$$

where $C_0 = 3.894\times10^5$ nb$\cdot$GeV^2 is a unit conversion factor, C_1 is the continuum free parameter, and ϕ_k is the phase angle among different components. The relativistic BW amplitude for a resonance $R_k \to D^{*0}D^{*-}\pi^+$ is written as

$${\rm BW}_k(\sqrt{s}) = \frac{m_k}{\sqrt{s}}\,\frac{\sqrt{12\pi\,\Gamma^{ee}_k\,\mathcal{B}_k\,\Gamma^{\rm tot}_k}}{s-m_k^2+im_k\Gamma^{\rm tot}_k}\,\sqrt{\frac{\Phi(\sqrt{s})}{\Phi(m_k)}},$$

where m_k and $\Gamma^{\rm tot}_k$ are the kth resonance mass and total width, respectively, $\Gamma^{ee}_k\cdot\mathcal{B}_k$ is the leptonic width of the kth resonance times the BF of $R_k \to D^{*0}D^{*-}\pi^+$, and $\Phi(\sqrt{s})$ is the three body phase space contribution defined as $\Phi(\sqrt{s}) = \iint[1/(2\pi)^3 32(\sqrt{s})^3]dm^2_{23}dm^2_{12}$ [1].

The χ^2 of the fit to the dressed cross section line shape is constructed according to the method in Ref. [68] by incorporating both the statistical and systematic uncertainty and considering both the correlated and uncorrelated terms. To avoid biasing the χ^2 minimization, the correlated uncertainties are calculated according to the predicted cross section values times the corresponding relative uncertainties when constructing the covariance matrix [69].

The fit result is shown in Fig. 3. There are eight solutions with the same fit quality with identical continuum contributions as well as masses and widths for the resonances [57]. However, the resulting product $\Gamma^{ee}_k\mathcal{B}_k$ and phases ϕ_k are different, as plotted in Fig. 2 of the Supplemental Material [54]. The numerical results are listed in Table I. In general, the magnitudes of $\Gamma^{ee}_k\mathcal{B}_k$ become increased when the destructive interference effects due to relative phase

TABLE I. The fit results of the dressed cross section line shape of $e^+e^- \to D^{*0}D^{*-}\pi^+$ with eight different solutions, which have the same fit quality as shown in Fig. 2 in the Supplemental Material [54]. For the uncertainties of the masses and widths, those from the solutions with maximum uncertainties are adopted.

	I	II	III	IV	V	VI	VII	VIII
$C_1(10^{-3})$				4.2 ± 1.5				
m_1 (MeV/c^2)				4209.6 ± 4.7				
$\Gamma_1^{\rm tot}$ (MeV)				81.6 ± 17.8				
$\Gamma_1^{ee}\mathcal{B}_1$ (eV)	5.4 ± 1.1	6.0 ± 1.3	4.8 ± 0.9	5.3 ± 1.1	17.9 ± 7.2	19.8 ± 6.6	20.2 ± 7.4	22.4 ± 9.0
ϕ_1 (rad)	3.1 ± 0.5	3.8 ± 0.4	1.9 ± 0.7	2.6 ± 0.6	4.2 ± 0.3	4.8 ± 0.2	5.4 ± 0.3	6.0 ± 0.3
m_2 (MeV/c^2)				4469.1 ± 26.2				
$\Gamma_2^{\rm tot}$ (MeV)				246.3 ± 36.7				
$\Gamma_2^{ee}\mathcal{B}_2$ (eV)	243.3 ± 83.5	832.5 ± 716.5	107.4 ± 50.6	367.4 ± 370.8	225.5 ± 94.9	770.8 ± 383.8	510.1 ± 202.3	1744.3 ± 926.9
ϕ_2 (rad)	4.4 ± 0.3	-0.9 ± 0.3	2.6 ± 0.6	3.7 ± 0.8	1.9 ± 0.8	3.0 ± 0.4	3.7 ± 0.3	-1.5 ± 0.3
m_3 (MeV/c^2)				4675.3 ± 29.5				
$\Gamma_3^{\rm tot}$ (MeV)				218.3 ± 72.9				
$\Gamma_3^{ee}\mathcal{B}_3$ (eV)	75.8 ± 148.8	1601.9 ± 1152.6	19.4 ± 27.1	411.6 ± 230.5	24.4 ± 34.5	515.6 ± 244.6	95.1 ± 173.1	2005.3 ± 1166.1
ϕ_3 (rad)	4.9 ± 1.4	-2.9 ± 0.4	2.1 ± 0.4	0.6 ± 1.1	1.7 ± 0.5	6.5 ± 0.5	4.5 ± 1.3	-3.3 ± 0.3

angles are larger. The dressed cross sections are also fitted under the assumption of only two resonances plus the continuum component. The relative changes in the χ^2 value ($\Delta\chi^2 = 130.5$) and the number of degrees of freedom (Δndof $= 4$) are used to estimate the significance of the three-resonance hypothesis over the two-resonance hypothesis as 10.8σ. The significance of the two-resonance hypothesis over the one-resonance hypothesis is 22.8σ according to the changes of $\Delta\chi^2 = 537.1$ and Δndof $= 4$.

The systematic uncertainties of the resonance parameters are dominated by those from the center-of-mass energy calibration, beam energy spread, and parametrization of the continuum contribution. Other uncertainties from the measured cross sections have been included in the line shape fit. The uncertainty from the center-of-mass energy measurement is estimated by propagating the largest uncertainty of the measured energies (0.8 MeV/c^2) to the ψ-state mass parameter. The uncertainty from beam energy spread is considered by smearing the energy with its spread value at each energy point. The differences of resonance parameters determined from fits using nominal and smeared line shapes are taken as the systematic uncertainties. To estimate the uncertainty related to the fit model, the three body continuum contribution is replaced by a third-order polynomial parametrized function. The resulting differences in the masses and widths of resonances are taken as systematic uncertainties. The total systematic uncertainty is obtained by summing the individual values in quadrature, assuming they are all uncorrelated, as listed in Table II.

TABLE II. The systematic uncertainties in the measurements of the ψ-state parameters.

Source	Energy	Beam spread	Fit model	Total
m_1 (MeV/c^2)	0.8	5.5	2.0	5.9
$\Gamma_1^{\rm tot}$ (MeV)	⋯	1.7	8.8	9.0
m_2 (MeV/c^2)	0.8	3.5	0.7	3.6
$\Gamma_2^{\rm tot}$ (MeV)	⋯	6.9	6.4	9.4
m_3 (MeV/c^2)	0.8	1.5	3.1	3.5
$\Gamma_3^{\rm tot}$ (MeV)	⋯	7.4	5.7	9.3

In summary, the Born cross sections of the process $e^+e^- \to D^{*0}D^{*-}\pi^+$ at 86 center-of-mass energies from $\sqrt{s} = 4.189$ to 4.951 GeV are measured for the first time with the data samples collected by the BESIII detector. Fitting the dressed cross sections with a three-resonance hypothesis, their masses and widths are determined to be $m_1 = 4209.6 \pm 4.7 \pm 5.9\,\text{MeV}/c^2$, and $\Gamma_1 = 81.6 \pm 17.8 \pm 9.0$ MeV [denoted as $\psi(4210)$], $m_2 = 4469.1 \pm 26.2 \pm 3.6$ MeV/c^2, and $\Gamma_2 = 246.3 \pm 36.7 \pm 9.4$ MeV [denoted as $\psi(4470)$], $m_3 = 4675.3 \pm 29.5 \pm 3.5$ MeV/c^2, and $\Gamma_3 = 218.3 \pm 72.9 \pm 9.3$ MeV [denoted as $\psi(4660)$], where the first uncertainties are statistical and the second are systematic. The significance of the three-resonance hypothesis compared with the two-resonance one is greater than 10σ. The mass of $\psi(4210)$ is consistent with the mass of $\psi(4230)$ from the combined fit in Ref. [39]. If we assume they are the same resonance, $\Gamma^{ee}_{\psi(4230)}$ becomes greater than 40 eV, which disfavors the hybrid interpretation under the lattice QCD calculation [38]. In addition, we find the couplings of $\psi(4230)$ to $D^{*0}D^{*-}\pi^+$ and $D^0D^{*-}\pi^+$ are at the same order of magnitude. This is the first observation of the state $\psi(4470)$ in an open-charm process, and its resonance parameters are compatible with those of the $\psi(4500)$ state observed in $e^+e^- \to K^+K^-J/\psi$ [24]. Assuming the $\psi(4470)$ and $\psi(4500)$ are the same state, the rate of its decay to $D^*\bar{D}^*\pi$ is 2 orders of magnitude greater than that to $K\bar{K}J/\psi$, which is inconsistent with the

conjectured hidden-strangeness tetraquark nature of the $\psi(4500)$ [40,42,44]. We confirm for the first time the existence of the resonance $\psi(4660)$ in open-charm final states with resonance parameters consistent with the latest results derived in $e^+e^- \to \pi^+\pi^-\psi(2S)$ at BESIII [14]. However, the relative size of their couplings cannot be constrained by current data, as different fit solutions result in large variations of the product $\Gamma^{ee}_{\psi(4660)}\mathcal{B}_{\psi(4660)}$. Further amplitude analyses of different open- and hidden-charm final states are desired to advance our knowledge of the nature of these charmoniumlike ψ states.

The BESIII Collaboration thanks the staff of BEPCII and the IHEP computing center for their strong support. This work is supported in part by the National Key R&D Program of China under Contracts No. 2020YFA0406400 and No. 2020YFA0406300; the National Natural Science Foundation of China (NSFC) under Contracts No. 11635010, No. 11735014, No. 11835012, No. 11935015, No. 11935016, No. 11935018, No. 11961141012, No. 12022510, No. 12025502, No. 12035009, No. 12035013, No. 12061131003, No. 12192260, No. 12192261, No. 12192262, No. 12192263, No. 12192264, No. 12192265, No. 12221005; the Chinese Academy of Sciences (CAS) Large-Scale Scientific Facility Program; the CAS Center for Excellence in Particle Physics (CCEPP); Joint Large-Scale Scientific Facility Funds of the NSFC and CAS under Contract No. U1832207; CAS Key Research Program of Frontier Sciences under Contracts No. QYZDJ-SSW-SLH003 and No. QYZDJ-SSW-SLH040; 100 Talents Program of CAS; Fundamental Research Funds for the Central Universities, Lanzhou University, University of Chinese Academy of Sciences; The Institute of Nuclear and Particle Physics (INPAC) and Shanghai Key Laboratory for Particle Physics and Cosmology; ERC under Contract No. 758462; European Union's Horizon 2020 research and innovation program under the Marie Sklodowska-Curie grant agreement under Contract No. 894790; the German Research Foundation DFG under Contracts No. 443159800 and No. 455635585, Collaborative Research Center CRC 1044, FOR5327, GRK 2149; Istituto Nazionale di Fisica Nucleare, Italy; Ministry of Development of Turkey under Contract No. DPT2006K-120470; the National Research Foundation of Korea under Contract No. NRF-2022R1A2C1092335; the National Science and Technology fund; the National Science Research and Innovation Fund (NSRF) via the Program Management Unit for Human Resources & Institutional Development, Research and Innovation under Contract No. B16F640076; the Polish National Science Centre under Contract No. 2019/35/O/ST2/02907; Suranaree University of Technology (SUT), Thailand Science Research and Innovation (TSRI), and National Science Research and Innovation Fund (NSRF) under Contract No. 160355; The Royal Society, UK under Contract No. DH160214; The Swedish Research Council; U.S. Department of Energy under Contract No. DE-FG02-05ER41374.

[a]Also at the Moscow Institute of Physics and Technology, Moscow 141700, Russia.
[b]Also at the Novosibirsk State University, Novosibirsk 630090, Russia.
[c]Also at the NRC "Kurchatov Institute," PNPI, 188300 Gatchina, Russia.
[d]Also at Goethe University Frankfurt, 60323 Frankfurt am Main, Germany.
[e]Also at Key Laboratory for Particle Physics, Astrophysics and Cosmology, Ministry of Education; Shanghai Key Laboratory for Particle Physics and Cosmology; Institute of Nuclear and Particle Physics, Shanghai 200240, People's Republic of China.
[f]Also at Key Laboratory of Nuclear Physics and Ion-beam Application (MOE) and Institute of Modern Physics, Fudan University, Shanghai 200443, People's Republic of China.
[g]Also at State Key Laboratory of Nuclear Physics and Technology, Peking University, Beijing 100871, People's Republic of China.
[h]Also at School of Physics and Electronics, Hunan University, Changsha 410082, China.
[i]Also at Guangdong Provincial Key Laboratory of Nuclear Science, Institute of Quantum Matter, South China Normal University, Guangzhou 510006, China.
[j]Also at Frontiers Science Center for Rare Isotopes, Lanzhou University, Lanzhou 730000, People's Republic of China.
[k]Also at Lanzhou Center for Theoretical Physics, Lanzhou University, Lanzhou 730000, People's Republic of China.
[l]Also at the Department of Mathematical Sciences, IBA, Karachi, Pakistan.

[1] R. L. Workman (Particle Data Group), Prog. Theor. Exp. Phys. **2022**, 083C01 (2022).
[2] B. Aubert *et al.* (*BABAR* Collaboration), Phys. Rev. Lett. **95**, 142001 (2005).
[3] Q. He *et al.* (CLEO Collaboration), Phys. Rev. D **74**, 091104 (2006).
[4] C. Z. Yuan *et al.* (Belle Collaboration), Phys. Rev. Lett. **99**, 182004 (2007).
[5] M. Ablikim *et al.* (BESIII Collaboration), Phys. Rev. Lett. **118**, 092001 (2017).
[6] M. Ablikim *et al.* (BESIII Collaboration), Phys. Rev. D **102**, 012009 (2020).
[7] M. Ablikim *et al.* (BESIII Collaboration), Phys. Rev. D **106**, 072001 (2022).
[8] B. Aubert *et al.* (*BABAR* Collaboration), Phys. Rev. Lett. **98**, 212001 (2007).
[9] J. P. Lees *et al.* (*BABAR* Collaboration), Phys. Rev. D **89**, 111103 (2014).
[10] X. L. Wang *et al.* (Belle Collaboration), Phys. Rev. Lett. **99**, 142002 (2007).
[11] X. L. Wang *et al.* (Belle Collaboration), Phys. Rev. D **91**, 112007 (2015).

[12] M. Ablikim *et al.* (BESIII Collaboration), Phys. Rev. D **96**, 032004 (2017); **99**, 019903(E) (2019).
[13] M. Ablikim *et al.* (BESIII Collaboration), Phys. Rev. D **97**, 052001 (2018).
[14] M. Ablikim *et al.* (BESIII Collaboration), Phys. Rev. D **104**, 052012 (2021).
[15] M. Ablikim *et al.* (BESIII Collaboration), Phys. Rev. Lett. **118**, 092002 (2017).
[16] M. Ablikim *et al.* (BESIII Collaboration), Phys. Rev. Lett. **114**, 092003 (2015).
[17] M. Ablikim *et al.* (BESIII Collaboration), Phys. Rev. D **99**, 091103 (2019).
[18] M. Ablikim *et al.* (BESIII Collaboration), Phys. Rev. D **102**, 031101 (2020).
[19] M. Ablikim *et al.* (BESIII Collaboration), Phys. Rev. D **101**, 012008 (2020).
[20] M. Ablikim *et al.* (BESIII Collaboration), Phys. Rev. Lett. **122**, 102002 (2019).
[21] M. Ablikim *et al.* (BESIII Collaboration), Phys. Rev. Lett. **129**, 102003 (2022).
[22] M. Ablikim *et al.* (BESIII Collaboration), Phys. Lett. B **804**, 135395 (2020).
[23] M. Ablikim *et al.* (BESIII Collaboration), Phys. Rev. D **106**, 052012 (2022).
[24] M. Ablikim *et al.* (BESIII Collaboration), Chin. Phys. C **46**, 111002 (2022).
[25] H. X. Chen, W. Chen, X. Liu, and S. L. Zhu, Phys. Rep. **639**, 1 (2016).
[26] F. K. Guo, C. Hanhart, U. G. Meißner, Q. Wang, Q. Zhao, and B. S. Zou, Rev. Mod. Phys. **90**, 015004 (2018); **94**, 029901(E) (2022).
[27] C. Z. Yuan, Natl. Sci. Rev. **8**, nwab182 (2021).
[28] J. Z. Bai *et al.* (BES Collaboration), Phys. Rev. Lett. **88**, 101802 (2002).
[29] R. A. Briceno *et al.*, Chin. Phys. C **40**, 042001 (2016).
[30] M. Ablikim *et al.* (BESIII Collaboration), J. High Energy Phys. 05 (2022) 155.
[31] M. Cleven, Q. Wang, F. K. Guo, C. Hanhart, U. G. Meißner, and Q. Zhao, Phys. Rev. D **90**, 074039 (2014).
[32] G. J. Ding, Phys. Rev. D **79**, 014001 (2009).
[33] G. Li and X. H. Liu, Phys. Rev. D **88**, 094008 (2013).
[34] M. T. Li, W. L. Wang, Y. B. Dong, and Z. Y. Zhang, arXiv: 1303.4140.
[35] Q. Wang, C. Hanhart, and Q. Zhao, Phys. Rev. Lett. **111**, 132003 (2013).
[36] X. G. Wu, C. Hanhart, Q. Wang, and Q. Zhao, Phys. Rev. D **89**, 054038 (2014).
[37] T. Ji, X. K. Dong, F. K. Guo, and B. S. Zou, Phys. Rev. Lett. **129**, 102002 (2022).
[38] Y. Chen, W. F. Chiu, M. Gong, L. C. Gui, and Z. Liu, Chin. Phys. C **40**, 081002 (2016).
[39] J. Zhang, L. Yuan, and R. Wang, Adv. High Energy Phys. **2018**, 5428734 (2018).
[40] T. W. Chiu *et al.* (TWQCD Collaboration), Phys. Rev. D **73**, 094510 (2006).
[41] C. F. Qiao, J. Phys. G **35**, 075008 (2008).
[42] X. K. Dong, F. K. Guo, and B. S. Zou, Progr. Phys. **41**, 65 (2021).
[43] Z. G. Wang, Nucl. Phys. **B973**, 115592 (2021).
[44] F. Z. Peng, M. J. Yan, M. Sánchez Sánchez, and M. Pavon Valderrama, Phys. Rev. D **107**, 016001 (2023).
[45] J. Z. Wang and X. Liu, Phys. Rev. D **107**, 054016 (2023).
[46] M. Ablikim *et al.* (BESIII Collaboration), Phys. Rev. Lett. **126**, 102001 (2021).
[47] M. Ablikim *et al.* (BESIII Collaboration), Phys. Rev. Lett. **129**, 112003 (2022).
[48] M. Ablikim *et al.* (BESIII Collaboration), Chin. Phys. C **41**, 063001 (2017).
[49] M. Ablikim *et al.* (BESIII Collaboration), Chin. Phys. C **45**, 103001 (2021).
[50] M. Ablikim *et al.* (BESIII Collaboration), Chin. Phys. C **46**, 113003 (2022).
[51] C. H. Yu *et al.*, *Proceeding of International Particle Accelerator Conference (IPAC'16), Busan, Korea* (JACoW, Geneva, Switzerland, 2016).
[52] M. Ablikim *et al.* (BESIII Collaboration), Nucl. Instrum. Methods Phys. Res., Sect. A **614**, 345 (2010).
[53] M. Ablikim *et al.* (BESIII Collaboration), Chin. Phys. C **44**, 040001 (2020).
[54] See Supplemental Material at http://link.aps.org/supplemental/10.1103/PhysRevLett.130.121901 for additional analysis information, which includes Refs. [1,48–50,55–57].
[55] M. Ablikim *et al.* (BESIII Collaboration), Phys. Rev. D **83**, 112005 (2011).
[56] M. Ablikim *et al.* (BESIII Collaboration), Phys. Rev. D **81**, 052005 (2010).
[57] Y. Bai and D. Y. Chen, Phys. Rev. D **99**, 072007 (2019).
[58] H. D. Jin, L. P. Zhou, B. X. Zhang, and H. M. Hu, Chin. Phys. C **43**, 013104 (2019).
[59] S. Agostinelli *et al.* (GEANT4 Collaboration), Nucl. Instrum. Methods Phys. Res., Sect. A **506**, 250 (2003).
[60] K. X. Huang, Z. J. Li, Z. Qian, J. Zhu, H. Y. Li, Y. M. Zhang, S. S. Sun, and Z. Y. You, Nucl. Sci. Tech. **33**, 142 (2022).
[61] S. Jadach, B. F. L. Ward, and Z. Was, Phys. Rev. D **63**, 113009 (2001); Comput. Phys. Commun. **130**, 260 (2000).
[62] D. J. Lange, Nucl. Instrum. Methods Phys. Res., Sect. A **462**, 152 (2001); R. G. Ping, Chin. Phys. C **32**, 599 (2008).
[63] J. C. Chen, G. S. Huang, X. R. Qi, D. H. Zhang, and Y. S. Zhu, Phys. Rev. D **62**, 034003 (2000); R. L. Yang, R. G. Ping, and H. Chen, Chin. Phys. Lett. **31**, 061301 (2014).
[64] E. Richter-Was, Phys. Lett. B **303**, 163 (1993).
[65] M. Ablikim *et al.* (BESIII Collaboration), Phys. Rev. Lett. **112**, 132001 (2014).
[66] F. Jegerlehner, Nuovo Cimento C **034S1**, 31 (2011).
[67] W. Sun, T. Liu, M. Jing, L. Wang, B. Zhong, and W. Song, Front. Phys. **16**, 64501 (2021).
[68] M. Ablikim *et al.* (BESIII Collaboration), Phys. Rev. D **103**, 072007 (2021).
[69] W. M. Sun, Nucl. Instrum. Methods Phys. Res., Sect. A **556**, 325 (2006).